

# TOPress3D: 3D topology optimization with design-dependent pressure loads in MATLAB

Prabhat Kumar<sup>1</sup>

*Department of Mechanical and Aerospace Engineering, Indian Institute of Technology Hyderabad, 502285, India*

*Department of Computational Engineering, Indian Institute of Technology Hyderabad, 502285, India*  
*Department of Engineering Science, Indian Institute of Technology Hyderabad, 502285, India*

Published<sup>2</sup> in *Optimization and Engineering*, DOI:10.1007/s11081-024-09931-2  
Submitted on 11 April 2024, Revised on 26 August 2024, Accepted on 20 September 2024

---

**Abstract:** This paper introduces “TOPress3D,” a 3D topology optimization MATLAB code for structures subjected to design-dependent pressure loads. With a primary focus on pedagogical objectives, the code provides an easy learning experience, making it a valuable tool and practical gateway for newcomers, students, and researchers towards this topic. TOPress3D uses Darcy’s law with a drainage term to link the given pressure load to design variables that, in turn, is converted to consistent nodal loads. Optimization problems focused on compliance minimization under volume constraints with pressure loads are solved. Load sensitivities arising due to design-dependent nature of the loads are evaluated using the adjoint-variable approach. The method of moving asymptotes is used to update the design variables. TOPress3D is constituted by six main parts. Each is described in detail. The code is also tailored to solve different problems. The robustness and success of the code are demonstrated in designing a few pressure load-bearing structures. The code is provided in Appendix B and is available with extensions in the supplementary material and publicly at <https://github.com/PrabhatIn/TOPress3D>.

**Keywords:** Topology optimization, Design-dependent pressure loads, MATLAB code, 3D compliance minimization problems

---

## 1 Introduction

This paper introduces “TOPress3D,” a MATLAB code (158 line) designed for performing 3D topology optimization on structures subjected to design-dependent fluidic pressure loads. While such loads are prevalent in various applications, addressing them within a topology optimization framework presents distinct challenges as they change direction, location and/or magnitude with design evolution (Hammer and Olhoff, 2000; Kumar et al., 2020). These challenges become more pronounced for 3D problems (Kumar and Langelaar, 2021). Therefore, availability of a publicly accessible pedagogical code can become particularly valuable and can serve as an educational tool and a practical entry point for newcomers, students, and researchers looking to familiarize themselves with this subject. TOPress3D is developed to fill the gap and accomplish the above mentioned objectives.

These days, topology optimization (TO) has become a widely used technique in various applications, as it provides efficient and innovative optimized designs. The technique solves the associated boundary value problems typically using finite element methods, wherein the design domain is discretized by finite elements (FEs), ranging from simple FEs such as triangles, quadrilaterals (Sigmund, 2001), and

---

<sup>1</sup>[pkumar@mae.iith.ac.in](mailto:pkumar@mae.iith.ac.in)

<sup>2</sup>This pdf is the personal version of an article whose final publication is available at [Optimization and Engineering](#)

hexahedral FEs (Amir et al., 2014; Liu and Tovar, 2014) to more advanced ones like honeycomb (hexagonal) tessellations (Saxena, 2011; Kumar, 2023a), polygonal elements (Talischi et al., 2012; Kumar and Saxena, 2015), and truncated octahedral FEs (Chi et al., 2020; Singh et al., 2024). A design variable  $\rho \in [0, 1]$  is assigned to each element that determines its state.  $\rho = 0$  indicates void phase, whereas  $\rho = 1$  denotes solid phase of the element. Depending on the nature of the loads, TO approaches can be classified into those with and without design-dependent loads. While many TO approaches exist for the latter, only a few methods have been reported for the former (Picelli et al., 2019; Kumar et al., 2020). The number of methods further reduces when considering 3D settings (Kumar and Langelaar, 2021). One may find 3D approaches only in Du and Olhoff (2004); Zhang et al. (2010); Yang et al. (2005); Sigmund and Clausen (2007); Wang and Qian (2020); Kumar and Langelaar (2021). In addition, a 3D paper with related code does not exist yet. Therefore, the current endeavor aims to potentially eliminate barriers hindering the learning and development of 3D TO with design-dependent loads and their extensions for solving different applications experiencing such loads, e.g., pneumatically actuated soft grippers (Pinskiar et al., 2023, 2024), pressure-loaded meta-materials, to name a few.

Making publicly available education codes in TO is a welcomed trend, which helps the technique grow faster and provides valuable tools. This trend is well accepted in academia and industry, which was started by Sigmund while presenting the first TO educational code having 99-line in MATLAB (Sigmund, 2001). Following the trend, many 2D educational papers with codes have been presented for different applications. A list of such codes can be found in Wang et al. (2021). On the other hand, the number of 3D TO papers with code is few, e.g., in Liu and Tovar (2014); Amir et al. (2014); Amir (2015); Aage et al. (2015); Lagaros et al. (2019); Chi et al. (2020); Ferrari and Sigmund (2020); Schmidt and Schulz (2011); Deng et al. (2021); Zuo and Xie (2015); Fernández et al. (2019); Smith and Norato (2020); Wang and Kang (2021); Du et al. (2022); Zhao et al. (2023); Zhuang et al. (2023); Kim et al. (2022). In addition, one cannot find such a publicly available code for 3D TO with design-dependent pressure loads. The motif herein is to fill the gap, benefiting students, researchers, and practitioners to delve into 3D TO with design-dependent loads and use and extend the provided code (TOPress3D) for different applications.

TOPress3D employs 3D hexahedral elements to parameterize design domains. It incorporates the 3D version of the Darcy law, including the drainage term described in Kumar and Langelaar (2021), to establish relationship between the given pressure load and design variables. The 2D counterpart of this relationship is available in Kumar et al. (2020) and related MATLAB code in Kumar (2023b). The variable naming conventions and framework within TOPress3D follow TOPress (Kumar, 2023b). The method of moving asymptotes (MMA, cf. Svanberg (1987)) is utilized for updating the design variables in the optimization process. MMA readily permits the code extension with additional physical/geometrical constraints, if any. The assembly process mentioned in Ferrari and Sigmund (2020) is used for handling the symmetric matrices (stiffness and flow matrices) of TOPress3D for efficiency. Whereas, noting that the transformation matrix (Sec. 2) is independent of the design variables, is assembled once before the optimization and used within the optimization process.

To summarize, this paper offers TOPress3D MATLAB code with the following new aspects:

- The code is developed with 3D hexahedral elements and made publicly available to optimize 3D load-bearing structures with design-dependent pressure loads for researchers, students, and newcomers to this area. It serves as an accessible gateway for extending the code to exciting applications, such as the design of pneumatically activated soft grippers or pressure-loaded meta-materials. In addition, it allows for the inclusion of the advanced constraints, such as buckling and stress, as needed for more complex applications.
- The code employs efficient assembly procedures outlined in Ferrari and Sigmund (2020) leveraging the symmetry in the elemental stiffness matrix ( $\mathbf{K}_e$ ) as well as the elemental flow matrices for Darcy ( $\mathbf{K}_p$ ) and drainage ( $\mathbf{K}_{Dp}$ ) using assembly matrices  $\mathbf{iK}$ ,  $\mathbf{jK}$ ,  $\mathbf{iP}$ ,  $\mathbf{jP}$  (Appendix B). To further reduce memory requirements, the code uses `fsparse` function (Engblom and Lukarski, 2016),

which requires `integer` precision, instead of `sparse` function that needs `double` precision. As a result, the displacement and pressure DOFs are stored as integers (Appendix B). This facilitates solving 3D problems on a laptop with a reasonable mesh grid.

- The code assembles the transformation matrix (Sec. 2) only once before the optimization loop, noticing that the elemental part of it is independent of the design variables using the respective assembly matrices `iT`, `jT` (Appendix B).
- The code contains six main parts, each explained in detail. Its various extensions are also presented.
- Code’s robustness and efficacy are demonstrated by solving four different design-dependent pressure loadbearing structures.

The remainder of the paper is organized as follows. Sec. 2 presents topology optimization framework—pressure field evaluation, consistent nodal load calculation, and optimization problem formulation with sensitivity analysis. Sec. 3 outlines MATLAB implementation of `TOPress3D` in detail and provides its various extensions. The numerical results for loadbearing structures are presented in Sec. 4. Lastly, Sec. 5 outlines the concluding remarks.

## 2 Topology optimization framework

For completeness, this section briefly outlines pressure load modeling, nodal load evaluation, and nomenclature/parameters’ values used in the code. Additionally, it mentions the objective formulation and sensitivity analysis for a compliance problem with a volume constraint. Readers are referred to [Kumar and Langelaar \(2021\)](#) for a more detailed description.

### 2.1 Pressure field evaluation

According to [Kumar et al. \(2020\)](#), Darcy’s law with a drainage term provides an elegant approach to model pressure load in a TO framework. The method has been successfully utilized to solve various problems, including 3D structures and compliant mechanism problems ([Kumar and Langelaar, 2021](#)), length-scale informed pressure-actuated compliant mechanisms ([Kumar and Langelaar, 2022](#)), a PneuNet of a soft robot ([Kumar, 2022](#)), with a featured-based method to obtain close to 0-1 topologies ([Kumar and Saxena, 2022](#)), multi-material grippers ([Pinsker et al., 2023, 2024](#)), multi-material frequency-constrained TO with polygonal FEs ([Banh et al., 2024](#)), multi-material structures with honeycomb tessellation ([Kumar, 2024](#)), and pneumatically actuated soft robots ([Kumar, 2023c](#)). The material states of elements change as TO progresses, i.e., one can consider characteristics of elements like porous media at the beginning with known pressure differences. To this end, Darcy’s flux  $\mathbf{q}$  is defined as ([Kumar et al., 2020](#))

$$\mathbf{q} = -\frac{\kappa}{\mu}\nabla p = -K(\tilde{\boldsymbol{\rho}})\nabla p, \quad (1)$$

where  $\nabla p$ ,  $\kappa$ , and  $\mu$  indicate the pressure gradient, permeability of the medium, and the fluid viscosity, respectively.  $\tilde{\boldsymbol{\rho}}$  represents the physical design vector. It is also the filtered design vector ([Bruns and Tortorelli, 2001](#)) corresponding to the design vector  $\boldsymbol{\rho}$  herein.  $K(\tilde{\boldsymbol{\rho}})$ , flow coefficient, is defined in terms of  $\tilde{\boldsymbol{\rho}}$ ; thus,  $\boldsymbol{\rho}$ , to relate the pressure field to the design vector. Mathematically,  $K(\tilde{\boldsymbol{\rho}})$  for element  $e$  is written as

$$K(\tilde{\rho}_e) = K_v (1 - (1 - \epsilon)\mathcal{H}(\tilde{\rho}_e, \beta_\kappa, \eta_\kappa)), \quad (2)$$

where  $\epsilon = \frac{K_s}{K_v}$  represents the flow contrast.  $K_v$  and  $K_s$  indicate the flow coefficients of void and solid phases of an element, respectively, and

$$\mathcal{H}(\tilde{\rho}_e, \beta_\kappa, \eta_\kappa) = \frac{\tanh(\beta_\kappa \eta_\kappa) + \tanh(\beta_\kappa(\tilde{\rho}_e - \eta_\kappa))}{\tanh(\beta_\kappa \eta_\kappa) + \tanh(\beta_\kappa(1 - \eta_\kappa))} \quad (3)$$

is a smooth Heaviside function. We write  $\{\eta_\kappa, \beta_\kappa\}$  the flow parameters (Kumar, 2023b), where  $\eta_\kappa$  and  $\beta_\kappa$  indicate the step position and slope of  $K(\tilde{\rho}_e)$ , respectively. We set  $K_v = 1$ , and  $\epsilon = 1 \times 10^{-7}$ , i.e.,  $K_s = \epsilon$  in TOPress3D code.  $K(\tilde{\rho}_e)$  is defined as (Kumar et al., 2020)

$$K(\tilde{\rho}_e) = 1 - (1 - \epsilon)\mathcal{H}(\tilde{\rho}_e, \beta_\kappa, \eta_\kappa). \quad (4)$$

The equilibrium equation corresponding to Eq. 1 is (Kumar et al., 2020)

$$\nabla \cdot \mathbf{q} = -\nabla \cdot (K(\tilde{\rho})\nabla p) = 0. \quad (5)$$

A drainage term is included in Darcy's law (Eq. 1) to achieve a realistic pressure field (Kumar and

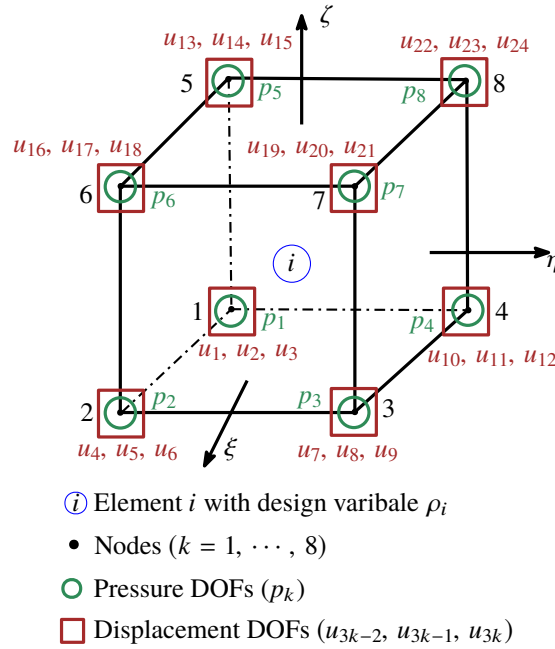


Figure 1: Element  $i$  nomenclature. Lface, Rface, Bface, Tface, Fface and Bface represent left, right, bottom, top, front, and back faces, respectively. Herein, these faces respectively contain  $\{1, 2, 5, 6\}$ ,  $\{3, 4, 7, 8\}$ ,  $\{1, 2, 3, 4\}$ ,  $\{5, 6, 7, 8\}$ ,  $\{2, 3, 6, 7\}$  and  $\{1, 4, 5, 8\}$  nodes.

Langelaar, 2021). As a result, Eq. 5 transpires to

$$\nabla \cdot \mathbf{q} - Q_{\text{drain}} = \nabla \cdot (K(\tilde{\rho})\nabla p) + Q_{\text{drain}} = 0, \quad (6)$$

with  $Q_{\text{drain}} = -D(\tilde{\rho}_e)(p - p_{\text{ext}})$ , where  $D(\tilde{\rho}_e) = D_s \mathcal{H}(\tilde{\rho}_e, \beta_d, \eta_d)$ .  $\{\eta_d, \beta_d\}$ , termed the drainage parameters, are analogous to  $\{\eta_\kappa, \beta_\kappa\}$ . To restrict the user-defined parameters, TOPress3D code considers  $\eta_d = \eta_\kappa = \eta_f$  and  $\beta_d = \beta_\kappa = \beta_f$ . In addition, users are free to select these parameters as per the recommendation provided in Kumar et al. (2020).

$$D_s = \left(\frac{\ln r}{\Delta s}\right)^2 K_s, \text{ with } r = \frac{p|_{\Delta s}}{p_{\text{in}}}, \quad (7)$$

where  $\Delta s$ , a penetration parameter, is set equal to size of a few FEs.  $p|_{\Delta s}$  indicates the pressure at  $\Delta s$ . One can use  $r \in [0.001 \ 0.1]$  (Kumar, 2023b).

As mentioned, the code uses hexahedral elements (Fig. 1) to describe the design domain. A hexahedral element with node numbers is displayed in Fig. 1. With standard finite element method (FEM), Eq. 6 is written as (Kumar and Langelaar, 2021)

$$\left[ \int_{\Omega_e} \left( K \mathbf{B}_p^\top \mathbf{B}_p \right) dV + \int_{\Omega_e} \left( D \mathbf{N}_p^\top \mathbf{N}_p \right) dV \right] \mathbf{p}_e = \mathbf{0}, \quad (8)$$

while considering  $p_{\text{out}} = 0$  and  $\mathbf{q}_\Gamma = \mathbf{0}$ .  $\mathbf{N}_p = [N_1, N_2, N_3, \dots, N_8]$  are the trilinear shape functions (Appendix A) for the hexahedral elements (Fig. 1),  $\mathbf{B}_p^\top = \nabla \mathbf{N}_p$ , and  $\mathbf{p}_e = [p_1, p_2, p_3, \dots, p_8]^\top$ . Note that  $N_k$  and  $p_k$  ( $k = 1, \dots, 8$ ) indicate shape function and pressure degree of freedom for the  $k^{\text{th}}$  node of hexahedral element  $i$ , respectively (Fig. 1). To this end, Eq. (8) yields to

$$\mathbf{K}_p^e \mathbf{p}_e + \mathbf{K}_{Dp}^e \mathbf{p}_e = \mathbf{A}_e \mathbf{p}_e = \mathbf{0}, \quad (9)$$

where element flow matrices of the Darcy and drainage parts are  $\mathbf{K}_p^e$  and  $\mathbf{K}_{Dp}^e$ , respectively. They are evaluated and their numerical value are provided in Appendix A.  $\mathbf{A}_e = \mathbf{K}_p^e + \mathbf{K}_{Dp}^e$  is the overall element flow matrix. Upon assembly, Eq. 9 yields to

$$\mathbf{A} \mathbf{p} = \mathbf{0}. \quad (10)$$

Since  $\mathbf{K}_p^e$  and  $\mathbf{K}_{Dp}^e$  are symmetric matrices; thus,  $\mathbf{A}$  is also a symmetric matrix. Eq. 10 is solved while applying the given pressure load boundary conditions.  $\mathbf{A}$  and  $\mathbf{p}$  are sub-blocked into free and prescribed pressure DOFs, denoted by subscripts  $f$  and  $p$ , respectively; Eq. 10 is rewritten as (Kumar, 2023c)

$$\begin{bmatrix} \mathbf{A}_{ff} & \mathbf{A}_{fp} \\ \mathbf{A}_{fp}^\top & \mathbf{A}_{pp} \end{bmatrix} \begin{bmatrix} \mathbf{p}_f \\ \mathbf{p}_p \end{bmatrix} = \begin{bmatrix} \mathbf{0} \\ \mathbf{0} \end{bmatrix} \quad (11)$$

Eq. 11 results in the following equations for free and prescribed pressure DOFs

$$\mathbf{A}_{ff} \mathbf{p}_f + \mathbf{A}_{fp} \mathbf{p}_p = \mathbf{0}, \quad (12)$$

and

$$\mathbf{A}_{fp}^\top \mathbf{p}_f + \mathbf{A}_{pp} \mathbf{p}_p = \mathbf{0}, \quad (13)$$

respectively. Since  $\mathbf{p}_p$  is known,  $\mathbf{p}_f$  is determined using Eq. 12 yielding  $\mathbf{p}_f = \mathbf{A}_{ff}^{-1} \mathbf{A}_{fp} \mathbf{p}_p$ . In TOPress3D code, we use the MATLAB `decomposition` function (line 123) to perform the above operations and compute  $\mathbf{p}_f$ . To verify the accuracy of  $\mathbf{p}_f$ , one can substitute it back into Eq. 13, which is typically necessary when using an indirect method to solve Eq. 12 for determining  $\mathbf{p}_f$ . Finally, one gets the pressure field  $\mathbf{p}$  as a function of physical variables (design variables) as  $\mathbf{p}_f$  is now known.

## 2.2 Nodal load evaluation

The pressure field  $\mathbf{p}$  is transformed into nodal loads by applying equilibrium conditions on an elemental cube experiencing body forces (Kumar et al., 2020; Kumar and Langelaar, 2021). We get (Kumar et al., 2020)

$$\mathbf{b} dV = -\nabla p dV, \quad (14)$$

where  $dV$  and  $\mathbf{b}$  indicate elemental volume and body force per unit volume, respectively. Given standard FEM, the nodal force  $\mathbf{F}_e$  for an element is determined as (Kumar and Langelaar, 2021)

$$\begin{aligned} \mathbf{F}_e &= \int_{\Omega_e} \mathbf{N}_u^\top \mathbf{b} dV = - \int_{\Omega_e} \mathbf{N}_u^\top \nabla p dV \\ &= - \left[ \int_{\Omega_e} \mathbf{N}_u^\top \mathbf{B}_p dV \right] \mathbf{p}_e = \mathbf{T}_e \mathbf{p}_e, \end{aligned} \quad (15)$$

where  $\mathbf{N}_{\mathbf{u}} = [N_1\mathbf{I}, N_2\mathbf{I}, N_3\mathbf{I}, \dots, N_8\mathbf{I}]$ , with  $\mathbf{I}$  the identity matrix in  $\mathcal{R}^3$ .  $\mathbf{F}_e$  is assembled to achieve its global nodal force vector  $\mathbf{F}$ . Expression and numerical value for  $\mathbf{T}_e$  are provided in Appendix A. Eq. 14 transpires to

$$\mathbf{F} = -\mathbf{T}\mathbf{p}, \quad (16)$$

in the global sense.  $\mathbf{T}$  is the global transformation matrix. Note that  $\mathbf{T}_e$  is independent of design variables; thus,  $\mathbf{T}$  is assembled prior to the optimization steps. This step helps save computational requirements; thus, making code relatively efficient.

### 2.3 Objective and sensitivity analysis

We solve the following optimization problem for the three-dimensional loadbearing structures with a given volume constraint:

$$\left. \begin{array}{l} \min_{\tilde{\boldsymbol{\rho}}} C(\tilde{\boldsymbol{\rho}}) = \mathbf{u}^\top \mathbf{K}(\tilde{\boldsymbol{\rho}})\mathbf{u} = \sum_{j=1}^{nel} \mathbf{u}_j^\top \mathbf{k}_j(\tilde{\rho}_j)\mathbf{u}_j \\ \text{subjected to:} \\ \quad \boldsymbol{\lambda}_1 : \mathbf{A}\mathbf{p} = \mathbf{0} \\ \quad \boldsymbol{\lambda}_2 : \mathbf{K}\mathbf{u} = \mathbf{F} = -\mathbf{T}\mathbf{p} \\ \quad \Lambda : V(\tilde{\boldsymbol{\rho}}) - V^* \leq 0 \\ \quad \mathbf{0} \leq \tilde{\boldsymbol{\rho}} \leq \mathbf{1} \\ \text{Data: } V^*, E_0, E_{\min}, p, K_v, \epsilon, \eta_f, \beta_f \end{array} \right\}, \quad (17)$$

where  $C$  and  $nel$  denote the structure's compliance and total number of elements used to represent design domain ( $\Omega_e$ ).  $\mathbf{K}$  is the global stiffness matrix, whereas  $\mathbf{u}$  indicates the global displacement vector.  $\mathbf{k}_j$  and  $\mathbf{u}_j$  are stiffness matrix and displacement vector for element  $j$ , respectively.  $V^*$  and  $V$  denote the permitted and current volume of  $\Omega_e$ , respectively.  $\mathbf{F}$  indicates the global force vector.  $\boldsymbol{\lambda}_1$ ,  $\boldsymbol{\lambda}_2$  and  $\Lambda$  are the Lagrange multipliers. The former two are vectors, whereas the latter one is a scalar. Vector  $\tilde{\boldsymbol{\rho}}$  represent filtered counterparts of design variable vector  $\boldsymbol{\rho}$ . The first vector is termed the physical vector herein.

One determines filtered design variable for element  $i$  as:

$$\tilde{\rho}_i = \frac{\sum_{j=1}^{nel} \rho_j v_j w(\mathbf{x}_i, \mathbf{x}_j)}{\sum_{j=1}^{nel} v_j w(\mathbf{x}_i, \mathbf{x}_j)}, \quad (18)$$

where  $w(\mathbf{x}_i, \mathbf{x}_j) = \max\left(0, 1 - \frac{\|\mathbf{x}_i - \mathbf{x}_j\|}{r_{\text{fill}}}\right)$  (Bruns and Tortorelli, 2001),  $r_{\text{fill}}$  and  $v_j$  are filter radius and volume of element  $j$ , respectively. One can determine  $v_j$  and  $w(\mathbf{x}_i, \mathbf{x}_j)$  prior to the optimization and can store in a matrix  $\mathbf{H}$  as:

$$\mathbf{H}_{i,j} = \frac{v_j w(\mathbf{x}_i, \mathbf{x}_j)}{\sum_{k=1}^{nel} v_k w(\mathbf{x}_i, \mathbf{x}_k)}. \quad (19)$$

The filtered design vector and its derivative with respect to the design vector can be written as  $\tilde{\boldsymbol{\rho}} = \mathbf{H}\boldsymbol{\rho}$  and  $\frac{\partial \tilde{\boldsymbol{\rho}}}{\partial \boldsymbol{\rho}} = \mathbf{H}^\top$ , respectively. TOPress3D uses `imfilter` MATLAB function for the filtering operations (see Appendix B).

The modified Solid Isotropic Material with Penalization (SIMP) interpolation scheme is used. Young's modulus of element  $i$ ,  $E_i$ , is written as

$$E_i = E_{\min} + \tilde{\rho}_i^p (E_1 - E_{\min}), \quad (20)$$

where  $p$  is the SIMP parameter.  $E_1$  and  $E_{\min}$  are Young's moduli of element's solid and void states, respectively.

### 2.3.1 Sensitivity analysis

We use the method of moving asymptotes (MMA, cf. [Svanberg \(1987\)](#)), a gradient-based optimizer, for updating the design variables. Thus, we need objective's and constraint's derivatives with respect to the design variables, which are determined using the adjoint-variable method herein. The augmented performance function  $\mathcal{L}$  in terms of objective function and equilibrium equations (17) can be written as ([Kumar, 2023b](#))

$$\mathcal{L} = \mathbf{u}^\top \mathbf{K} \mathbf{u} + \boldsymbol{\lambda}_1^\top \mathbf{A} \mathbf{P} + \boldsymbol{\lambda}_2^\top (\mathbf{K} \mathbf{U} + \mathbf{T} \mathbf{P}). \quad (21)$$

Equation (21) is differentiated with respect to the physical design variable, and rearranging, one gets

$$\begin{aligned} \frac{d\mathcal{L}}{d\tilde{\rho}_i} = & \mathbf{u}^\top \frac{\partial \mathbf{K}}{\partial \tilde{\rho}_i} \mathbf{u} + \boldsymbol{\lambda}_2^\top \left( \frac{\partial \mathbf{K}}{\partial \tilde{\rho}_i} \mathbf{u} \right) + \boldsymbol{\lambda}_1^\top \left( \frac{\partial \mathbf{A}}{\partial \tilde{\rho}_i} \mathbf{P} \right) \\ & + \underbrace{\left( 2\mathbf{u}^\top \mathbf{K} + \boldsymbol{\lambda}_2^\top \mathbf{K} \right)}_{\Xi_1} \frac{\partial \mathbf{u}}{\partial \tilde{\rho}_i} + \underbrace{\left( \boldsymbol{\lambda}_1^\top \mathbf{A} + \boldsymbol{\lambda}_2^\top \mathbf{T} \right)}_{\Xi_2} \frac{\partial \mathbf{P}}{\partial \tilde{\rho}_i} \end{aligned} \quad (22)$$

One use  $\Xi_1 = 0$  and  $\Xi_2 = 0$  to determine  $\boldsymbol{\lambda}_1$  and  $\boldsymbol{\lambda}_2$  from the above equation, i.e.,

$$\begin{aligned} \boldsymbol{\lambda}_2 &= -2\mathbf{u}, \\ \boldsymbol{\lambda}_1^\top &= -\boldsymbol{\lambda}_2^\top \mathbf{T} \mathbf{A}^{-1} = 2\mathbf{u}^\top \mathbf{T} \mathbf{A}^{-1}, \end{aligned} \quad (23)$$

and, therefore,

$$\frac{dC}{d\tilde{\rho}_i} = -\mathbf{u}^\top \frac{\partial \mathbf{K}}{\partial \tilde{\rho}_i} \mathbf{u} + \underbrace{2\mathbf{u}^\top \mathbf{T} \mathbf{A}^{-1}}_{\text{Load sensitivities}} \frac{\partial \mathbf{A}}{\partial \tilde{\rho}_i} \mathbf{P} \quad (24)$$

Load sensitivities, appeared in Eq. (24) due to the design-dependent nature of the load, affect the optimized topologies as demonstrated in prior work such as [Kumar \(2023c\)](#); [Kumar et al. \(2020\)](#); [Kumar \(2023b\)](#). Therefore, neglecting them during optimization may not be advisable. Finally, using the chain rule, the objective derivatives can be determined ([Kumar, 2023b](#)). Calculation of the derivative of the volume constraint is straightforward ([Sigmund, 2001](#)). In the subsequent section, we provide the MATLAB implementation for TOPress3D code.

## 3 Structure of TOPress3D

The section provides a complete description of the MATLAB code, TOPress3D. Reader can download the code, provided in Appendix B, and its extensions from the supplementary material of the paper. One calls the code in the MATLAB command window as

```
TOPress3D(nelx, nely, nelz, volf, penal, rmin, etaf, betaf, lst, maxit)}
```

where `nelx`, `nely` and `nelz` indicate the number of elements in  $x$ -,  $y$ - and  $z$ -directions, respectively. `volf` represents the given volume fraction, `penal` refers to the penalty parameter of the SIMP technique (Eq. 20), `rmin` is the filter radius, `etaf` and `betaf` are related to the flow coefficient and drainage term, respectively. `lst` indicates the status of load-sensitivities. `lst = 1` indicates that load sensitivities are considered in the optimization process, whereas `lst = 0` means otherwise. `maxit` variable indicates the maximum number of MMA iterations. Hexahedral elements are used for discretizing the domains. Local degree of freedoms (DOFs) pertaining to displacement and pressure are shown in Fig. 1. TOPress3D contains the following six main parts:

### (I) MATERIAL AND FLOW PARAMETERS INITIALIZATION



- (II) FINITE ELEMENT ANALYSIS AND PASSIVE SOLID/VOID REGIONS PREPARATION
- (III) ASSIGNING PRESSURE B.Cs, DISPLACEMENT B.Cs, AND LAGRANGE MULTIPLIERS INITIALIZATION
- (IV) FILTER PREPARATION
- (V) MMA OPTIMIZATION PREPARATION AND INITIALIZATION
- (VI) MMA OPTIMIZATION LOOP
  - (VI.1) SOLVING FLOW BALANCED EQUATION
  - (VI.2) DETERMINING CONSISTENT NODAL LOADS AND GLOBAL DISPLACEMENT VECTOR
  - (VI.3) OBJECTIVE, CONSTRAINT AND THEIR SENSITIVITIES COMPUTATION
  - (VI.4) SETTING AND CALLING MMA OPTIMIZATION
  - (VI.5) PRINTING AND PLOTTING RESULTS

We describe each part in detail below:

(I) **MATERIAL AND FLOW PARAMETERS INITIALIZATION:** `E1` (line 3) and `Emin` (line 4) indicate  $E_1$  (Eq. 20) and  $E_{\min}$  (Eq. 20), respectively. Line 5 mentions Poisson’s ratio, `nu`, which is set to 0.30. On line 6, values of  $K_v$  (Eq. 2), indicated by `Kv`,  $\epsilon$  (Eq. 2), indicated by `epsf`,  $r$  and  $\Delta s$ , indicated by `De1s` (Eq. 7), are given utilizing `deal` MATLAB function. `deal` function creates multiple output variables with specified values.  $D_s$  and  $(K_v - K_s)$  are denoted by `Ds` and `Kvs`, respectively, and are determined on line 7.

(II) **FINITE ELEMENT ANALYSIS AND PASSIVE SOLID/VOID REGIONS PREPARATION:** This part provides FE analysis preparation for flow and structure parts of the code on lines 8-87. The part at end also facilitates the inclusion of passive solid/void regions, if any. Number of nodes in  $x$ -,  $y$ - and  $z$ -directions are recorded in `ndx`, `ndy` and `ndz`, respectively on line 9. `nel` and `nno` indicate the total number of FEs and nodes, respectively. `nel` and `nno` are determined on line 10. As node numbers and associated displacement and pressure DOFs are integers, we use `int32` MATLAB function while recording them. Instead of using `sparse` MATLAB function, we use `fsparse` routine, created by (Engblom and Lukarski, 2016) to perform the assembly procedure. The former records locations (DOFs-rows and columns) information as double precision numbers, whereas the latter records them as integers, thus saving computational requirements that, in turn, make the procedure computationally efficient (Ferrari and Sigmund, 2020). Next, we mention the procedure to use/install `fsparse`.

For using `fsparse`, one can download the “`stenglib`” library<sup>3</sup> and install it as per the `README.md` file. Extract the downloaded ‘`stenglib-master.zip`’ file, copy the folder “Fast” and make it the current folder in MATLAB and then type ‘make’ in the command windows and press ‘Enter’ bottom on the keyboard. If MATLAB requests to install ‘MinGW64 Compiler (C)’, download and install the said compiler and run ‘make’ again as procedure said earlier. Once the compilation is done, the user can see the ‘MEX-file’ in the “Fast” folder. One can then place `TOPress3D.m` code and its extensions with `mmasub.m` and `subsolv.m` files in ‘Fast’ folder and execute `TOPress3D.m` and its extensions as suggested in Sec. 4.

The matrix containing displacement DOFs, recorded in `Udofs`, is created on lines 13-14 using array `nodenrs` (line 11) and vector `edofVec` (line 12). Line 15 determines pressure DOFs, all pressure DOFs, and displacement DOFs. They are recorded in `Pdofs`, `allPdofs` and `allUdofs`, respectively. Nodes

<sup>3</sup><https://github.com/stefanengblom/stenglib>



constituting faces are determined next, as they are required to apply the given pressure loads. In that view, lines 16-18 determine nodes that form the bottom and top faces of domain in vectors `BTface` and `Tface`, respectively. In addition, nodes making the left and right faces are recorded on line 19 in vectors `Lface` and `Rface`, respectively. Further, line 20 determines nodes constituting the front and back faces in vectors `Fface` and `Bface`, respectively. Vectors `iK` and `jK`, required for performing assembly of the stiffness matrix, are determined on line 26 as per [Ferrari and Sigmund \(2020\)](#). To reduce the assembly indexing, `Iar` is determined on line 27, which is used on line 127. Lines 28-51 record the lower half of the elemental stiffness matrix in vector `Ke`. `Ke` is used for the assembling the stiffness matrix on line 127; also, to recover the complete elemental matrix `Ke0` on lines 52. `Ke0` (lines 52-54) is used to evaluate the compliance sensitivity on line 133. Following the above steps, vectors `iP` and `jP`, analogous to vectors `iK` and `jK`, are determined on line 59 for flow matrix assembly. `IarP` analogous to `Iar` is determined on line 60. Element flow matrix corresponding to the Darcy law (`Kp1`) and drainage term (`KDp1`), in the factorized form, are recorded on lines 61-62 and lines 63-64, respectively. `Kp1` and `KDp1` indicate  $\mathbf{K}_p^e$  and  $\mathbf{K}_{DP}^e$  (Eq. 9), respectively with unit  $K$  (Eq. 8) and  $D$  (Eq. 8) (see Appendix A). The corresponding full matrices `Kp` and `KDp` are recovered between lines 65-67. These matrices are needed while determining the load sensitivities (lines 134-136). Lengths of vectors `Ke` and `Kp1` are determined on line 68 utilizing, which are used later on lines 126 and line 117, respectively. On lines 69-75, the code records elemental transformation matrix  $\mathbf{T}_e$  (Eq. 15) in the vectorized form in vector `Te`. As `Te` is a rectangular matrix, the assembly procedure to determine the global transformation matrix  $\mathbf{T}$  (Eq. 16) is similar to `TOPress` code. Vectors `iT` and `jT` are created on lines 76 and 77, respectively. Noting that the transformation matrix is independent of the design variables, the global form  $\mathbf{T}$  (Eq. 16) is determined on line 79 and recorded in `TG`. This steps save computational requirements.

Smooth Heaviside projection function (Eq. 3), `IFprj`, needed to define the flow (Eq. 2) and drainage (Eq. 6) coefficients, is defined on lines 80-81. The function has three input variables. Lines 82-83 determine its derivative with respect to the first variable, i.e., the design variable, and recorded in a function `dIFprj`. The derivative function is required on lines 134-135 to determine the load sensitivities. Line 84 gives room to include passive solid (NDS)/void (NDV) regions, if any. Active design vector is determined on line 85 and is recorded in `act`.

**(III) ASSIGNING PRESSURE B.Cs, DISPLACEMENT B.Cs, AND LAGRANGE MULTIPLIERS INITIALIZATION:** This part of the code assigns pressure load and boundary conditions, displacement boundary conditions (fixed and free DOFs). This part also initializes the global displacement and  $\lambda_1$  (Eq. 23). On line 87, vector `PF` initializes pressure load vector, and scalar `Pin` contains the magnitude of the input pressure load. Line 88 updates `PF` as per the applied pressure loading locations. Fixed pressure DOFs, recorded in `fixedPdofs`, and free pressure DOFs, stored in `freePdofs`, are determined on line 89 and line 90, respectively. On line 91, array `fixeddofsv` records the fixed pressure DOFs and corresponding values in its first and second columns, respectively. Lines 92-93 record fixed displacement nodes in vector `fixnn`. Vector `fixedUdofs` stores fixed displacement DOFs (line 94). Free displacement DOFs are recorded in `freeUdofs` (line 95). The global displacement vector `U` and Lagrange multiplier `lam1` for the sensitive analysis are initialized on line 96.

**(IV) FILTER PREPARATION:** `imfilter` MATLAB function is used for performing the density filtering. The filter variable `Hs` is determined on lines 97-101. One can also determine the filter parameters as ([Amir et al., 2014](#); [Amir, 2015](#); [Liu and Tovar, 2014](#)):

```

iH = ones(nelx*nely*nelz*(2*(ceil(rmin)-1)+1)^3,1);
jH = ones(size(iH));
sH = zeros(size(iH));
k = 0;
for i1 = 1:nelx
    for k1 = 1:nelz
        for j1 = 1:nely
            e1 = (i1-1)*nely*nelz + (k1-1)*nely + j1;
            for i2 = max(i1-(ceil(rmin)-1),1):min(i1+(ceil(rmin)-1),nelx)

```

```

        for k2 = max(k1-(ceil(rmin)-1),1):min(k1+(ceil(rmin)-1),nelz)
            for j2 = max(j1-(ceil(rmin)-1),1):min(j1+(ceil(rmin)-1),nely)
                e2 = (i2-1)*nely*nelz + (k2-1)*nely + j2;
                k = k + 1;
                iH(k) = e1;
                jH(k) = e2;
                sH(k) = max(0,rmin-sqrt((i1-i2)^2+(j1-j2)^2+(k1-k2)^2));
            end
        end
    end
end
end
end
end
Hk = sparse(iH,jH,sH);
Hs = sum(Hk,2);

```

and replace line 109, line 140 and line 149 (right part) by

```
dVol = Hk*(dVol0./Hs);
```

```
objsens = Hk*(objsens*normf./Hs);
```

and

```
xphys = (Hk*xphys(:))./Hs;
```

respectively.

(V) **MMA OPTIMIZATION PREPARATION AND INITIALIZATION:** Lines 102-110 provide this part of the code. Line 103 initializes design variable vector  $\mathbf{x}$  and provides the unfiltered derivative of the volume constraint in vector  $\mathbf{dVol0}$ .  $\mathbf{x}$  is updated on line 104 using the active design variable vector  $\mathbf{act}$ .  $\mathbf{nMMA}$ ,  $\mathbf{mMMA}$ ,  $\mathbf{xphys}$ ,  $\mathbf{xMMA}$ , and  $\mathbf{mvLt}$  indicate the number of design variables, number of the constraints, physical design vector, design variable used in the MMA, and external move limit for the MMA, respectively. These variables are defined on line 105. Vectors  $\mathbf{xminvec}$  and  $\mathbf{xmaxvec}$  define the minimum and maximum value of the design vector (line 106). Lower ( $\mathbf{low}$ ) and upper ( $\mathbf{upp}$ ) values of the design vector are defined on line 107. The same line also initializes vectors  $\mathbf{xold1}$  and  $\mathbf{xold2}$ , which will be used to restore the old design vector during optimization. Other important parameters of the MMA, e.g.,  $\mathbf{cMMA}$ ,  $\mathbf{dMMA}$ ,  $\mathbf{a0}$  and  $\mathbf{aMMA}$  are defined on line 108 (Svanberg, 1987). The code uses 2007 version of the MMA code<sup>4</sup>. As density filtering is volume preserving, we perform filtering of the derivatives of the volume constraint above the optimization loop on line 109 in vector  $\mathbf{dVol}$ .  $\mathbf{loop}$  records the optimization loop, and  $\mathbf{change}$  tracks the absolute change in the design vector during optimization (line 110).

(VI) **MMA OPTIMIZATION LOOP:** The MMA optimization loop contains five parts, which starts with  $\mathbf{while}$  loop with termination conditions on  $\mathbf{maxit}$  and  $\mathbf{change}$ . Lines 111-158 describe this part of the code. Line 114 defines the definition of the  $\mathbf{while}$  loop.  $\mathbf{loop}$  is used to store the progress optimization's iterations line 113.

(VI.1) **SOLVING THE FLOW BALANCE EQUATION** (Lines 114-122): This part of the code provides the pressure field in terms of the physical (design) variables. The flow coefficients ( $K$ , cf. Eq. 2) and drainage coefficients ( $D$ , cf. Eq. 6) of all FEs are recorded in vectors  $\mathbf{Kc}$  (line 115) and  $\mathbf{Dc}$  (line 116), respectively. The elemental flow coefficient matrix due to the Darcy law and drainage term,  $\mathbf{A}_e$ , (Eq. 9) is determined on line 117 and recorded in  $\mathbf{Ae}$ . The global flow coefficient matrix,  $\mathbf{A}$  (Eq. 10), (in lower triangular form) is determined on line 118 using  $\mathbf{fsparse}$  and recorded in  $\mathbf{AG}$ . Line 119 determines the flow coefficient matrix corresponding to the

<sup>4</sup><https://www.smoptit.se/>

free pressure DOFs and records in `Aff`. The full matrix of `AG` is recovered on line 120. Line 121 determines pressure field,  $\mathbf{p}$  (Eq. 10), and stores in `PF`. We use `decomposition` MATLAB function with ‘`ldl`’ type and ‘`lower`’ format for determining `PF`. Pressure load vector `PF` is modified per the known pressure load conditions on line 122.

(VI.1) **DETERMINING CONSISTENT NODAL LOAD AND GLOBAL DISPLACEMENT VECTORS** (Lines 123-129): Line 124 provides global load vector `F` using matrix `TG` (line 79) and vector `PF` (line 122). Young’s modulus vector `E` is determined on line 125. The elemental stiffness matrix is stored in the vector form on line 126, which is further used for determining the global stiffness matrix `K` (Eq. 17) on line 127. The latter is stored in matrix `KG`. Cholesky factorization function `chol` is used on line 128. On line 129, the global displacement vector `U` is determined. One can also replace the direct solver with the multigrid-preconditioned CG (Amir et al., 2014; Amir, 2015) to obtain vectors `PF` and `U`.

(VI.3) **OBJECTIVE, CONSTRAINT AND THEIR SENSITIVITIES COMPUTATION** (Line 130-140): The objective is determined on line 131.  $\lambda_1$  is determined on line 132 and stored in `lam1`. Derivatives of the objective without load sensitivity terms are determined on line 133 and are stored in `objst1`. The load sensitivities are determined on line 136 using `dC1k` (line 134, contribution from the Darcy law) and `dC1d` (line 135, contribution from the drainage term) and are stored in a vector `objst2`. The final derivatives are determined on line 137 and are recorded in `objsens`. `1st` defines presence (`1st=1`) or absence (`1st=0`) of `objst2` in vector `objsens`. On line 138, the volume fraction of the intermediate design is determined in `Vol`. Normalization parameter `normf` is defined and determined on line 139. `normf` is utilized to normalize the objective; thus, the objective derivatives consistently. The vector `objsens` is filtered while normalizing on line 140.

(VI.4) **SETTING AND CALLING MMA OPTIMIZATION** (Lines 141-150): `xval` is initialized with `xMMA` on line 142. Vectors `xminvec` and `xmaxvec` are updated on line 143 using vector `xval` and parameter `mvLt`. The MMA subroutine `mmasub` is called on line 144, which updates the new design variable `xmma`. Vectors `xold1` and `xold2` are updated on line 146. A new design vector `xnew` is determined using `xmma` on line 148. `change` is determined on line 147 using the new and old design vectors. Line 148 also updates `xMMA` using `xnew`. On line 149, the physical design vector `xphys` is updated, and filtering is performed. Next line updates `xphys` using information for the solid and void passive regions.

(VI.5) **PRINTING AND PLOTTING RESULTS** (Lines 151-157): We print `loop`, objective value, volume fraction, and `change` on line 152 using `fprintf` MATLAB function. MATLAB functions `cla`, `shftdim`, `smooth3`, `patch`, `view`, `axis`, `drawnow` and `camlight` are used to plot the optimized results (Amir et al., 2014; Amir, 2015) between lines 153-157. On line 158, the `while` loop gets ended.

## 4 Results

We provide four examples of pressure loadbearing structures to demonstrate the versatility and robustness of `TOPress3D`. In the material and flow definition, we set  $E1 = 1$ ,  $E_{min} = E1 \times 10^{-5}$ ,  $\nu = 0.3$ ,  $Kv = 1$ ,  $\epsilon_{psf} = 10^{-7}$ ,  $r = 0.1$ , and  $De1s = 2$ . We use a 64-bit laptop with Processor Intel(R) Core(TM) i5-8265U 1.60 GHz, RAM 8GB, Windows 11 Pro, and MATLAB 2022a for presenting the numerical results herein.

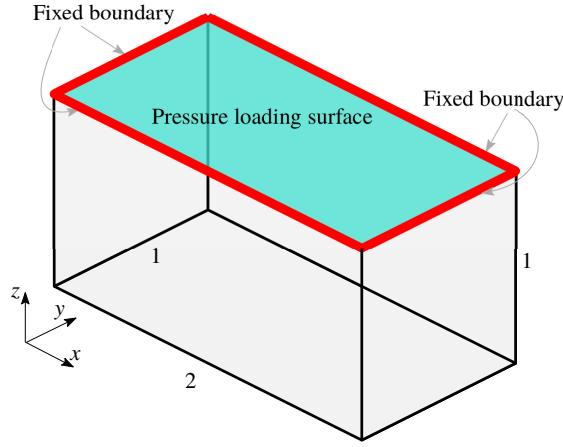


Figure 2: Design domain for a loadbearing lid structure. Pressure load is applied on the top surface, and all its edges are fixed.

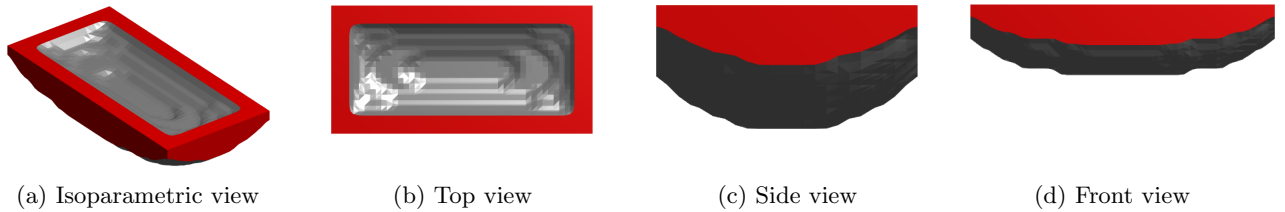


Figure 3: Optimized pressure loadbearing lid structure in different views. The domain is parameterized using  $48 \times 24 \times 24$  FEs. The density value of the isosurface displayed is 0.3

## 4.1 Loadbearing Lid Structure

The original state of `TOPress3D` is set for designing a pressure loadbearing lid structure (Fig. 2). The problem is reported earlier in [Du and Olhoff \(2004\)](#); [Sigmund and Clausen \(2007\)](#); [Zhang et al. \(2010\)](#); [Kumar and Langelaar \(2021\)](#).

The design domain, applied pressure load, and displacement boundary conditions are illustrated in Fig. 2. The top surface of the domain experiences pressure load, whereas the bottom face receives zero pressure loading. All edges of the top surface are fixed. Dimension of the domain is considered to be  $2 \times 1 \times 1$ . While the problem has symmetry with respect to the vertical planes, we use the entire domain to obtain the optimized design to notice any deviation from the symmetry.

We call `TOPress3D` in the MATLAB command windows as

```
TOPress3D(48,24,24,0.25,3,sqrt(3),0.20,10,1,100);
```

wherein  $nelx = 48$ ,  $nely = 24$ ,  $nelz = 24$ ,  $volf = 0.25$ ,  $rmin = \sqrt{3}$ ,  $etaf = 0.20$ ,  $betaf = 10$ ,  $lst = 1$ ,  $maxit = 100$ . The optimized loadbearing lid structure in different views is displayed in Fig. 3. The density value of the isosurface displayed is 0.3 for the optimized design (Fig. 3). Note that to obtain the top view, side view, and front view, one changes `view(3)` (line 159) to `view(90,90)`, `view(180,0)`, and `view(270,0)`, respectively. The obtained optimized design is symmetrical and provides a suitable chamber on the top surface to contain more fluid pressure while optimizing the strength of the design. The normalized-objective and volume fraction convergence histories are depicted in Fig. 4. One notices that changes in the objective and volume fraction are insignificant from the 20<sup>th</sup> iteration onwards. The volume constraint remains active at the end of the optimization.

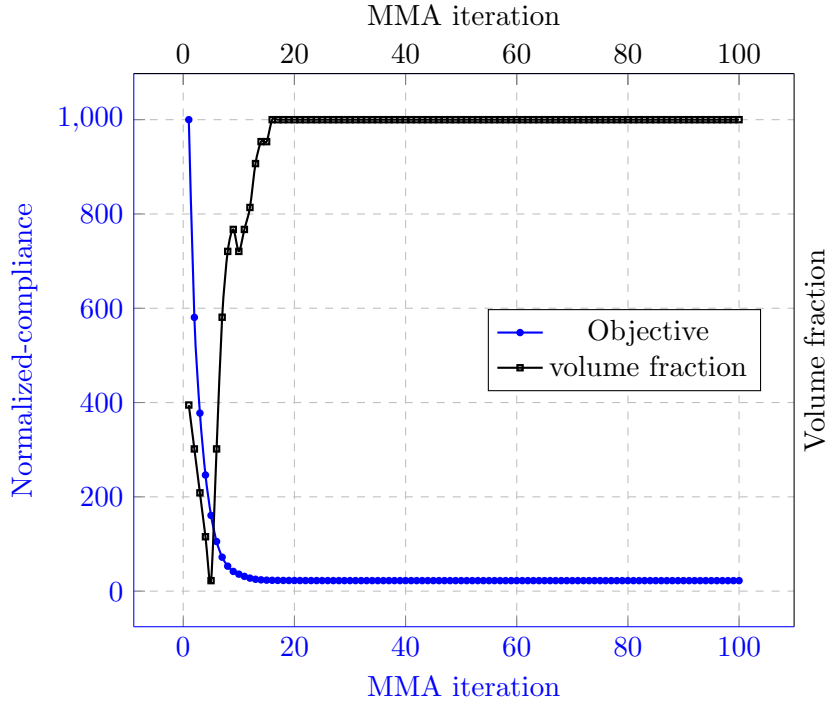


Figure 4: Convergence plot for the loadbearing lid structure

## 4.2 Externally Pressurized Structure

An externally pressurized structure is optimized. This particular problem is previously reported in [Kumar and Langelaar \(2021\)](#); [Zhang et al. \(2010\)](#); [Du and Olhoff \(2004\)](#). The design domain is depicted in Fig. 5. The top surface of the structure experiences a fluidic pressure load, while the left and right edges of the bottom face are fixed, as depicted in the figure. The left and right faces can slide in the  $z$ -direction. The bottom face get zero pressure loading. The dimensions of the domain are considered to be  $2 \times 1 \times 1$ . Note that the optimization, in this case, is focused exclusively on the right symmetric half part with respect to the  $yz$ -plane of the domain.

For applying the pressure load, line 88 is modified to

```
PF(BTface)= 0; PF(Tface) = Pin;
```

Boundary conditions are applied by replacing the lines 92-94 with the following code:

```
fixnn = intersect(BTface,Rface);
fixedUdofs = [3*fixnn-2 3*fixnn-1 3*fixnn 3*Lface-2 3*Rface-1 3*Rface-2] ;
```

In the plotting routine, one replaces line 153 with the following code to plot the full optimized design from the symmetrical half result:

```
cla; isovals = zeros(nelx*2,nely,nelz);
isovals(nelx+1:2*nelx,1:nely,1:nelz) = shiftdim(reshape(xphys,nely,nelz,nelx),2);
isovals(1:nelx,1:nely,1:nelz) = isovals(2*nelx:-1:nelx+1,1:nely,1:nelz);
```

With the above modifications TOPress3D code is called as

```
TOPress3D(36,36,36,0.25,3,sqrt(3),0.2,10,1,100);
```

with  $nelx = 36$ ,  $nely = 36$ ,  $nelz = 36$ ,  $vol_f = 0.25$ ,  $rmin = \sqrt{3}$ ,  $eta_f = 0.20$ ,  $beta_f = 10$ ,  $lst = 1$ ,  $maxit = 100$ .

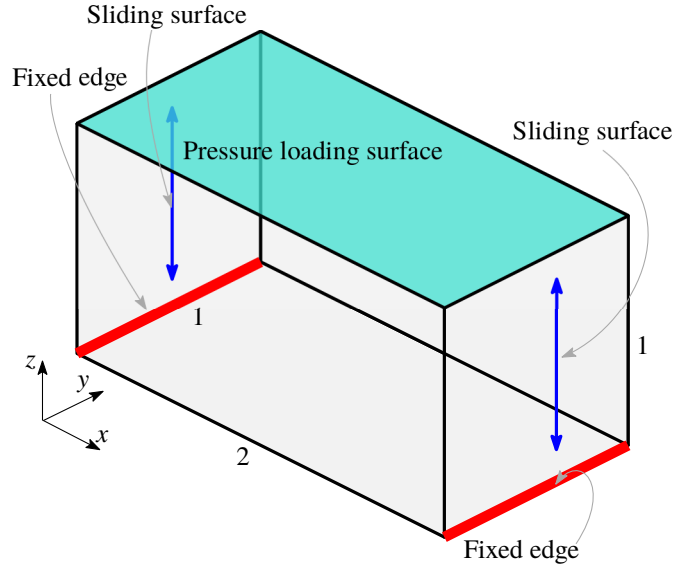


Figure 5: Design domain for an externally pressurized structure. The pressure load is applied on the top surface. The bottom, front and back faces get zero pressure loading. The left and right edges of the bottom face are fixed. The left and right faces slid in the vertical direction.

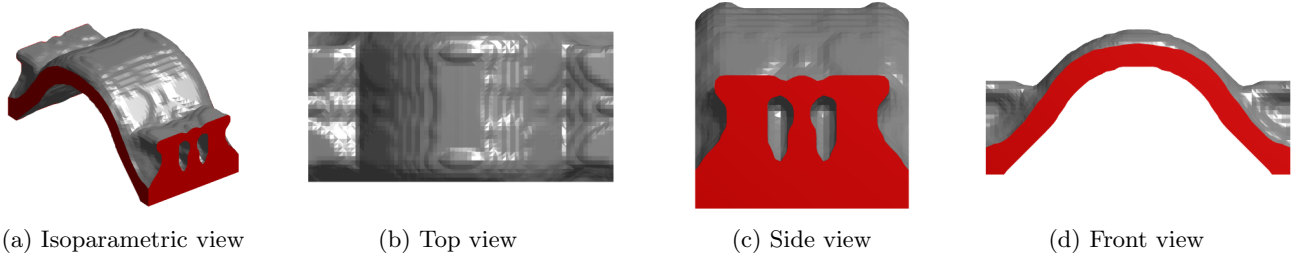


Figure 6: Optimized externally pressurized structure in different views. The symmetrical half domain is parameterized using  $36 \times 36 \times 36$  FEs. The density value of the isosurface displayed is 0.3

The optimized design with different views is illustrated in Fig. 6. The results are displayed with isosurface 0.3. The symmetrical half-optimized design is suitably converted into a full optimized design using the above plotting code. We find that convergences for the objective and volume constraint are smooth, and the volume constraint remains active at the end of the optimization.

### 4.3 Dam Structure

A dam structure, solved first in [Sigmund and Clausen \(2007\)](#), is optimized herein. The design domain is shown in Fig. 7. The pressure load is applied on the back face of the domain, whereas the front face experiences zero pressure load. The left, right, and bottom faces are fixed. Note that designing an actual dam structure requires complicated loading and boundary conditions ([Sigmund and Clausen, 2007](#)). The dimensions of the domain are  $2 \times 1 \times 1$ . Utilizing the symmetry of the problem, only one-half of the domain is optimized.

To solve this problem using `TOPress3D`, one modifies line 88 to

```
PF(Fface) = 0; PF(Bface) = Pin;
```

and line 92-94 to

```
fixnn = unique([BTface,Rface]);
fixedUdofs = [3*fixnn-2 3*fixnn-1 3*fixnn 3*Lface-2];
```

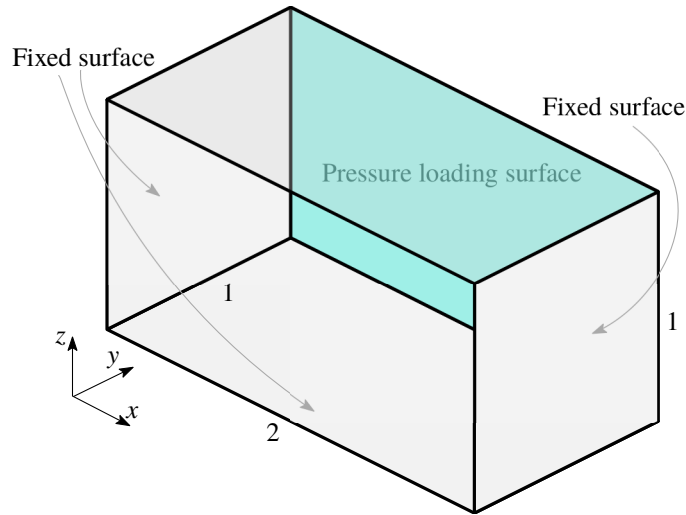


Figure 7: A Dam design domain. The bottom, left, and right faces are fixed. The back face experiences pressure load, whereas the front face receives no pressure load.

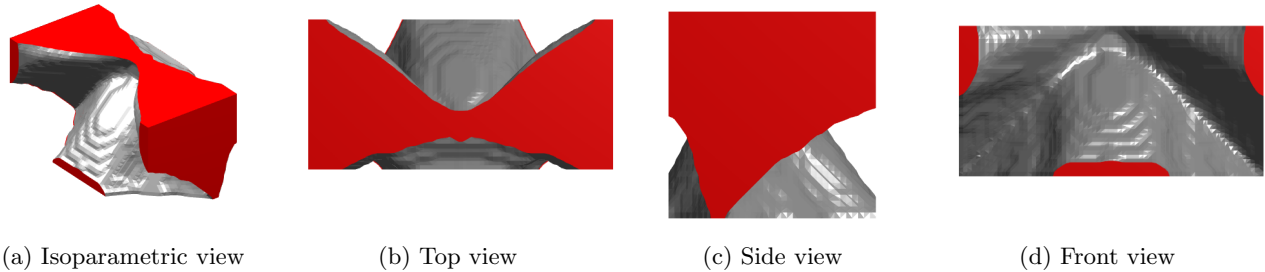


Figure 8: Optimized pressure loadbearing dam structure in different views. The symmetrical half domain is parameterized using  $36 \times 36 \times 36$  FEs. The density value of the isosurface displayed is 0.3

In the plotting, we perform a similar code presented for an externally pressurized structure. Having done the above modification, the user can call `TOPress3D` code as

```
TOPress3D(36,36,36,0.5,3,sqrt(3),0.2,10,1,100);
```

wherein  $nelx = 36$ ,  $nely = 36$ ,  $nelz = 36$ ,  $vol_f = 0.5$ ,  $rmin = \sqrt{3}$ ,  $etaf = 0.20$ ,  $betaf = 10$ ,  $lst = 1$ ,  $maxit = 100$ .

The optimized design in the full domain is shown in Fig. 8. Different views are also depicted in the figure. The optimized design resembles that presented in Sigmund and Clausen (2007). The convergence of optimization's progress is found to be smooth.

#### 4.4 Externally Pressurized hull structure

To demonstrate the code's capability with design domains having passive regions, we optimize a pressure hull structure herein (Wang and Qian, 2020). Fig. 9 depicts the design domain of the structure. All the surfaces are pressurized from the outside. The hull's center contains a cuboid passive void region, which is fixed (Fig. 9). The dimensions of the domain and void region are  $1 \times 1 \times 1$  and  $\frac{1}{9} \times \frac{1}{9} \times \frac{1}{9}$ , respectively. Note that one may change the size of the void as per the requirement.

One makes the following modifications in `TOPress3D` to solve this problem. Line 84 is replaced by

```
e1Nrs = reshape(1:nel,nely,nelz,nelx);
v1 = e1Nrs(8*nely/18:10*nely/18,8*nelz/18:10*nelz/18,8*nelx/18:10*nelx/18);
[NDS,NDV] = deal([], [v1(:)]);
```



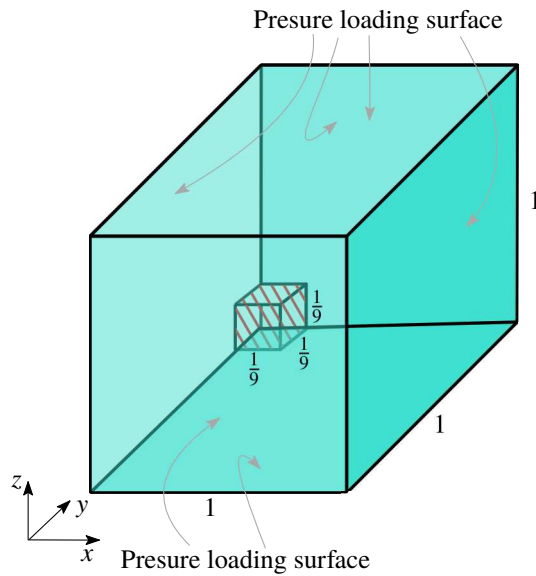


Figure 9: An externally pressurized hull structure. The structure is pressurized from all sides. A center cuboid void region is present, which is fixed.

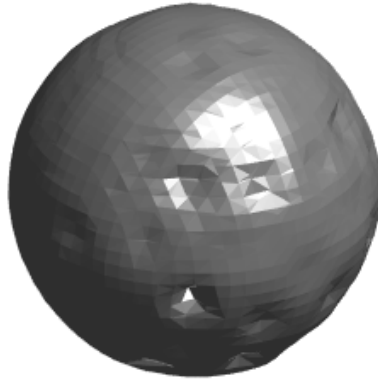


Figure 10: Optimized pressure loadbearing hull design.

```
Vnode = unique(Pdofs(v1(:),:));
```

where `eINrs` matrix arranges the element number in 3D matrix fashion using `reshape` MATLAB inbuilt function. `v1` extracts the information of FEs which are inside the void region (Fig. 9). Using `v1`, next, `NDV` is determined. Nodes constituting elements in `v1` are extracted in vector `Vnode` using matrix `Pdofs`. Now, to apply the pressure load, line 88 is changed to

```
PF(unique([BTface Bface Tface Fface Lface Rface])) = Pin; PF(Vnode(:)) = 0;
```

and boundary conditions are applied by changing lines 92-94 to

```
fixedUdofs = [ 3*Vnode(:)-2 3*Vnode(:)-1 3*Vnode(:)];
```

After performing the above modification, `TOPress3D` code is called as

```
TOPress3D(36,36,36,0.2,3,sqrt(3),0.2,10,1,100);
```

with `nelx = 36`, `nely = 36`, `nelz = 36`, `volf = 0.5`, `rmin =  $\sqrt{3}$` , `etaf = 0.20`, `betaf = 10`, `lst = 1`, `maxit = 100`.

The optimized pressure loadbearing hull structure is illustrated in Fig. 10. The optimized hull structure resembles that presented in Wang and Qian (2020). Smooth and steady convergence characteristics are noticed for the objective and volume fraction.

The working and success of the presented TOPress3D are demonstrated above in four examples. We envision that the code will allow people new to the 3D topology optimization field to learn and explore different applications. The code can also be extended to solve pressure loadbearing structures with advanced constraints, e.g., stress constraints, buckling constraints, etc.

## 5 Concluding remarks

This paper introduces a MATLAB code, TOPress3D, comprising 158 lines, for 3D topology optimization for structures with design-dependent pressure loads. While such loads are encountered in various applications, addressing them within a TO framework proves challenging due to the dynamic nature of their magnitude, direction, and location during (especially at the beginning of) the optimization process. These challenges are particularly more evident in 3D TO problems, potentially posing difficulties for newcomers and students on the learning path. The developed TOPress3D can become a valuable tool and practical gateway for individuals entering the field, including newcomers, students, and researchers. The code utilizes the method of moving asymptotes to update design variables. Darcy’s law with a drainage term is used to determine the pressure field in terms of the design values. The obtained pressure field is converted to consistent nodal loads.

The code (Appendix B) comprises six main subroutines, each explained in detail within the paper. Efficiency in matrix assembly is improved by representing mesh-related quantities as integers (MATLAB `int32`) and assembling only one half of the matrices. The transformation matrix is assembled before the optimization process, as its elemental part is independent of the design vector; which in turn saves computational time. To determine the state variables (pressure and displacement herein) one can also utilize the preconditioned iterative solvers as mentioned in TOPress3D.

The structure’s compliance is minimized with specified volume constraints. The efficacy and robustness of the code are demonstrated for designing four pressure loadbearing structures. The original state of TOPress3D is set for optimizing pressure loadbearing lid structure. The convergence plots for the objective and volume constraint are smooth. Extensions of the code are mentioned to solve different pressure loadbearing structures. We anticipate that the code will serve as a valuable platform for learning, development, and extension to diverse applications involving design-dependent loads and opens several possibilities for future research.

## Appendix A Determining $\mathbf{K}_p^e$ , $\mathbf{K}_{Dp}^e$ and $\mathbf{T}_e$

We provide the expressions for the flow matrices  $\mathbf{K}_p^e$  and  $\mathbf{K}_{Dp}^e$ , and transformation matrix  $\mathbf{T}_e$  for element  $e$ .

As mentioned, hexahedral FEs are used to describe the design domain. Each FE contains 8 nodes (Fig. 1). To interpolate the geometry, displacement field and pressure field, the Lagrange shape functions, noted below for the  $k$  – th node, are used (Zienkiewicz et al., 2005)

$$N_k = \frac{1}{8}(1 + \xi_k \xi)(1 + \eta_k \eta)(1 + \zeta_k \zeta); k = 1 \text{ to } 8 \quad (\text{A.1})$$

where  $(\xi_k, \eta_k, \zeta_k)$  represents the coordinates of node  $k$  of the element in the  $(\xi, \eta, \zeta)$  system (Fig. 1).

We note the following expressions of  $\mathbf{K}_p^e$ ,  $\mathbf{K}_{Dp}^e$  and  $\mathbf{T}_e$  for element  $e$  from Sec. 2 as

$$\begin{aligned}
\mathbf{K}_p^e &= \int_{\Omega_e} K \mathbf{B}_p^\top \mathbf{B}_p dV \\
&= \int_{-1}^{+1} \int_{-1}^{+1} \int_{-1}^{+1} \left( K \mathbf{B}_p^\top \mathbf{B}_p \right) |\det \mathbf{J}| d\xi d\eta d\zeta \\
\mathbf{K}_{Dp}^e &= \int_{\Omega_e} D \mathbf{N}_p^\top \mathbf{N}_p dV \\
&= \int_{-1}^{+1} \int_{-1}^{+1} \int_{-1}^{+1} \left( D \mathbf{N}_p^\top \mathbf{N}_p \right) |\det \mathbf{J}| d\xi d\eta d\zeta \\
\mathbf{T}_i &= - \int_{\Omega_e} \mathbf{N}_u^\top \mathbf{B}_p dV \\
&= - \int_{-1}^{+1} \int_{-1}^{+1} \int_{-1}^{+1} \mathbf{N}_u^\top \mathbf{B}_p |\det \mathbf{J}| d\xi d\eta d\zeta
\end{aligned} \tag{A.2}$$

where we have used  $dV = |\det \mathbf{J}| d\xi d\eta d\zeta$  and  $\mathbf{J}$  is the  $(3 \times 3)$  Jacobian matrix. The integration is performed numerically using the Gauss quadrature (Zienkiewicz et al., 2005), that yields<sup>5</sup>

$$\mathbf{K}_p^e|_{K=1} = \frac{1}{12} \begin{bmatrix} 4 & & & & & & & & \\ 0 & 4 & & & & & & & \\ -1 & 0 & 4 & & & & & & \\ 0 & -1 & 0 & 4 & & & & & \\ 0 & -1 & -1 & -1 & 4 & & & & \\ -1 & 0 & -1 & -1 & 0 & 4 & & & \\ -1 & -1 & 0 & -1 & -1 & 0 & 4 & & \\ -1 & -1 & -1 & 0 & 0 & -1 & 0 & 4 & \end{bmatrix} \text{Sym.} \tag{A.3}$$

$$\mathbf{K}_{Dp}^e|_{D=1} = \frac{1}{216} \begin{bmatrix} 8 & & & & & & & & \\ 4 & 8 & & & & & & & \\ 2 & 4 & 8 & & & & & & \\ 4 & 2 & 4 & 8 & & & & & \\ 4 & 2 & 1 & 2 & 8 & & & & \\ 2 & 4 & 2 & 1 & 4 & 8 & & & \\ 1 & 2 & 4 & 2 & 2 & 4 & 8 & & \\ 2 & 1 & 2 & 4 & 4 & 2 & 4 & 8 & \end{bmatrix} \text{Sym.} \tag{A.4}$$

---

<sup>5</sup>The symbolic calculation is performed first, then using the coordinates of a unit cube; these matrices are determined in numerical forms.

$$\mathbf{T}_e = \frac{1}{72} \begin{bmatrix} -4 & 4 & 2 & -2 & -2 & 2 & 1 & -1 \\ -4 & -2 & 2 & 4 & -2 & -1 & 1 & 2 \\ -4 & -2 & -1 & -2 & 4 & 2 & 1 & 2 \\ -4 & 4 & 2 & -2 & -2 & 2 & 1 & -1 \\ -2 & -4 & 4 & 2 & -1 & -2 & 2 & 1 \\ -2 & -4 & -2 & -1 & 2 & 4 & 2 & 1 \\ -2 & 2 & 4 & -4 & -1 & 1 & 2 & -2 \\ -2 & -4 & 4 & 2 & -1 & -2 & 2 & 1 \\ -1 & -2 & -4 & -2 & 1 & 2 & 4 & 2 \\ -2 & 2 & 4 & -4 & -1 & 1 & 2 & -2 \\ -4 & -2 & 2 & 4 & -2 & -1 & 1 & 2 \\ -2 & -1 & -2 & -4 & 2 & 1 & 2 & 4 \\ -2 & 2 & 1 & -1 & -4 & 4 & 2 & -2 \\ -2 & -1 & 1 & 2 & -4 & -2 & 2 & 4 \\ -4 & -2 & -1 & -2 & 4 & 2 & 1 & 2 \\ -2 & 2 & 1 & -1 & -4 & 4 & 2 & -2 \\ -1 & -2 & 2 & 1 & -2 & -4 & 4 & 2 \\ -2 & -4 & -2 & -1 & 2 & 4 & 2 & 1 \\ -1 & 1 & 2 & -2 & -2 & 2 & 4 & -4 \\ -1 & -2 & 2 & 1 & -2 & -4 & 4 & 2 \\ -1 & -2 & -4 & -2 & 1 & 2 & 4 & 2 \\ -1 & 1 & 2 & -2 & -2 & 2 & 4 & -4 \\ -2 & -1 & 1 & 2 & -4 & -2 & 2 & 4 \\ -2 & -1 & -2 & -4 & 2 & 1 & 2 & 4 \end{bmatrix} \quad (\text{A.5})$$

## Appendix B The MATLAB code: TOPress3D

```

1 function TOPress3D(nelx,nely,nelz,volfrac,penal,rmin,etaf,betaf,lst,maxit)
2 %% ___PART 1.-----MATERIAL AND FLOW PARAMETERS
3 E1 = 1; % Youngs' Modulus of solid
4 Emin = E1*1e-5; % Youngs's Modulus of void
5 nu = 0.30; % Poisson's ratio
6 [Kv,epsf,r,Dels] = deal(1,1e-7,0.1,2); % Flow parameters
7 [Ds, Kvs]= deal((log(r)/Dels)^2*epsf,Kv*(1 - epsf)); % Flow parameters
8 %% ___PART 2.-----FINITE ELEMENT ANALYSIS PREPARATION and NON-DESIGN REGIONS
9 [ndx,ndy,ndz] = deal(nelx+1,nely+1,nelz+1); % Node number in x, y and z
10 [nel,nno] = deal(nelx*nely*nelz, ndx*ndy*ndz); % Number of elements and nodes
11 nodenrs = int32(reshape( 1 : nno,ndy, ndz, ndx ) );
12 edofVec = reshape( 3 * nodenrs( 1 : nely, 1 : nelz, 1 : nelx ) + 1, nel, 1);
13 Udofs = edofVec + int32( [0,1,2,3*ndy*ndz+[0,1,2,-3,-2,-1],-3,-2,-1,3*ndy+...
14 [0,1,2],3*ndy*(ndz+1)+[0,1,2,-3,-2,-1],3*ndy+[-3,-2,-1]]); % Displacement DOFs matrix
15 [Pdofs,allPdofs, allUdofs] = deal(Udofs(:,3:3:end)/3,1:nno,1:3*nno); % Press DOFs, all
    DOFs disp DOFs
16 Tface = (ndy*nelz+1:ndz*ndy:nno-nely)+ (0:nely)';
17 BTface=(1:ndz*ndy:nno-nely)+ (0:nely)';
18 [Tface, BTface] = deal(Tface(:)', BTface(:)');
19 [Lface,Rface] = deal((1:ndy*ndz), (ndy*ndz*nelx+1:nno)); % Det left and right faces
20 [Bface,Fface] = deal((ndy:ndy:nno), (1:ndy:nno-nely)); % Det front and back faces
21 [skI, skII, spI, spII] = deal( [ ] );
22 for j = 1 : 24
23 skI = cat( 2, skI, j : 24 );
24 skII = cat( 2, skII, repmat( j, 1, 24 - j + 1 ) );
25 end
26 [iK, jK ] = deal( Udofs( :, skI )', Udofs( :, skII )' );
27 Iar = sort( [ iK( : ), jK( : ) ], 2, 'descend' ); clear iK jK % Reduced assembly index
28 Ke = 1/(1+nu)/(2*nu-1)/144 *( [ -32;-6;-6;8;6;6;10;6;3;-4;-6;-3;-4;-3;-6;10;...
29 3;6;8;3;3;4;-3;-3; -32;-6;-6;-4;-3;6;10;3;6;8;6;-3;-4;-6;-3;4;-3;3;8;3;...
30 3;10;6;-32;-6;-3;-4;-3;-3;4;-3;-6;-4;6;6;8;6;3;10;3;3;8;3;6;10;-32;6;6;...
31 -4;6;3;10;-6;-3;10;-3;-6;-4;3;6;4;3;3;8;-3;-3;-32;-6;-6;8;6;-6;10;3;3;4;...
32 -3;3;-4;-6;-3;10;6;-3;8;3;-32;3;-6;-4;3;-3;4;-6;3;10;-6;6;8;-3;6;10;-3;...
33 3;8;-32;-6;6;8;6;-6;8;3;-3;4;-3;3;-4;-3;6;10;3;-6;-32;6;-6;-4;3;3;8;-3;...
34 3;10;-6;-3;-4;6;-3;4;3;-32;6;3;-4;-3;-3;8;-3;-6;10;-6;-6;8;-6;-3;10;-32;...
35 6;-6;4;3;-3;8;-3;3;10;-3;6;-4;3;-6;-32;6;-3;10;-6;-3;8;-3;3;4;3;3;-4;6;...
36 -32;3;-6;10;3;-3;8;6;-3;10;6;-6;8;-32;-6;6;8;6;-6;10;6;-3;-4;-6;3;-32;6;...
37 -6;-4;3;6;10;-3;6;8;-6;-32;6;3;-4;3;3;4;3;6;-4;-32;6;-6;-4;6;-3;10;-6;3;...
38 -32;6;-6;8;-6;-6;10;-3;-32;-3;6;-4;-3;3;4;-32;-6;-6;8;6;6;-32;-6;-6;-4;...
39 -3;-32;-6;-3;-4;-32;6;6;-32;-6;-32]+nu*[ 48;0;0;0;-24;-24;-12;0;-12;0;...
40 24;0;0;0;24;-12;-12;0;-12;0;0;-12;12;12;48;0;24;0;0;0;-12;-12;-24;0;-24;...
41 0;0;24;12;-12;12;0;-12;0;-12;-12;0;48;24;0;0;12;12;-12;0;24;0;-24;-24;0;...
42 0;-12;-12;0;0;-12;-12;0;-12;48;0;0;0;-24;0;-12;0;12;-12;12;0;0;0;-24;...
43 -12;-12;-12;-12;0;0;48;0;24;0;-24;0;-12;-12;-12;-12;12;0;0;24;12;-12;0;...
44 0;-12;0;48;0;24;0;-12;12;-12;0;-12;-12;24;-24;0;12;0;-12;0;0;-12;48;0;...
45 0;-24;24;-12;0;0;-12;12;-12;0;0;-24;-12;-12;0;48;0;24;0;0;0;-12;0;-12;...
46 -12;0;0;0;-24;12;-12;-12;48;-24;0;0;0;-12;12;0;-12;24;24;0;0;12;-12;...
47 48;0;0;-12;-12;12;-12;0;0;-12;12;0;0;0;24;48;0;12;-12;0;0;-12;0;-12;-12;...
48 -12;0;0;-24;48;-12;0;-12;0;0;-12;0;12;-12;-24;24;0;48;0;0;0;-24;24;-12;...
49 0;12;0;24;0;48;0;24;0;0;0;-12;12;-24;0;24;48;-24;0;0;-12;-12;-12;0;-24;...
50 0;48;0;0;0;-24;0;-12;0;-12;48;0;24;0;24;0;-12;12;48;0;-24;0;12;-12;-12;...
51 48;0;0;0;-24;-24;48;0;24;0;0;48;24;0;0;48;0;0;48;0;48 ] ); % Elem stiffness matrix
52 Ke0( tril( ones( 24 ) ) == 1 ) = Ke';
53 Ke0 = reshape( Ke0, 24, 24 );
54 Ke0 = Ke0 + Ke0' - diag( diag( Ke0 ) ); % Extracting full form
55 for j = 1 : 8
56 spI = cat( 2, spI, j : 8 );
57 spII = cat( 2, spII, repmat( j, 1, 8-j + 1 ) );
58 end
59 [iP, jP ] = deal( Pdofs( :, spI )', Pdofs( :, spII )' );
60 IarP = sort( [ iP( : ), jP( : ) ], 2, 'descend' ); clear iP jP

```

```

61 Kp1 = [4;0;-1;0;0;-1;-1;-1;4;0;-1;-1;0;-1;-1;4;0;-1;-1;0;-1;4;-1;-1;-1; ...
62 0;4;0;-1;0;4;0;-1;4;0;4]/12; % Flow matrix due to Darcy
63 KDp1 = [8;4;2;4;4;2;1;2;8;4;2;2;4;2;1;8;4;1;2;4;2;8;2;1;2;4;8;4;2;4;8;...
64 4;2;8;4;8]/216; % Flow matrix due to drainage term
65 [Kp(tril(ones(8))==1), KDp(tril(ones(8))==1)]= deal(Kp1',KDp1);
66 [Kp,KDp]= deal(reshape(Kp,8,8),reshape(KDp,8,8));
67 Kp = Kp + Kp' - diag(diag(Kp)); KDp = KDp + KDp' - diag(diag(KDp));
68 [lKe, lKp1] = deal(length(Ke), length(Kp1));
69 Te = [-4;-4;-4;-4;-2;-2;-2; -2; -1;
-2;-4;-2;-2;-2;-4;-2;-1;-2;-1;-1;-1;-1;-1;...
70 -2;-2;4;-2;-2;4;-4;-4;2;-4;-2;2;-2;-1;2;-1;-2;2;-2;-4;1;-2;-2;1;-1;-1;2;...
71 2;-1;2;4;-2;4;4;-4;4;2;-2;1;1;-1;1;2;-2;2;2;-4;2;1;-2;-2;4;-2;-2;2;-1;-4;...
72 2;-2;-4;4;-4;-1;2;-2;-1;1;-1;-2;1;-2;-2;2;-4;-2;-2;4;-2;-1;2;-1;-1;1;-1;...
73 -2;2;-4;-4;4;-4;-2;2;-2;-2;1;-2;-4;2;2;-1;2;2;-2;4;1;-2;2;1;-1;1;4;-2;2;...
74 4;-4;4;2;-4;2;2;-2;1;1;1;1;1;2;2;2;2;4;2;1;2;2;2;1;2;4;2;4;4;4;2;2;-1;...
75 2;2;-1;1;1;-2;1;2;-2;2;4;-2;4;2;-2;2;1;-4;2;2;-4;4;4]/72;
76 iT = reshape(kron(Udofs,int32(ones(8,1)))',192*nel,1);
77 jT = reshape(kron(Pdofs,int32(ones(1,24)))',192*nel,1);
78 Ts = reshape(Te(:)*ones(1,nel), 192*nel, 1); % Elemental transformation matrix
79 TG = fsparse(iT, jT, Ts); clear Te iT jT Ts % Global transformation matrix
80 IFprj=@(xv,etaf,betaf)((tanh(betaf*etaf) + tanh(betaf*(xv-etaf)))/... % Proj fun
81 (tanh(betaf*etaf) + tanh(betaf*(1 - etaf))));
82 dIFprj=@(xv,etaf,betaf) betaf*(1-tanh(betaf*(xv-etaf)).^2)...
83 /(tanh(betaf*etaf)+tanh(betaf*(1-etaf))); % Derivative of the projection function
84 [NDS, NDV ] = deal( [], [] );
85 act = setdiff((1 : nel)', union( NDS, NDV ));
86 %% ___PART 3._____PRESSURE & STRUCTURE B.C's, LOADS
87 [PF, Pin] =deal(0.00001*ones(nno,1),1); % Pressure-field preparation
88 PF(BTface) = 0; PF(Tface) = Pin; % Applying pressure load
89 fixedPdofs = allPdofs(PF~=0.00001); % Given P-dofs
90 freePdofs = setdiff(allPdofs,fixedPdofs); % Free P-dofs
91 pfixeddofsv = [fixedPdofs' PF(fixedPdofs)]; % p-fixed and its value
92 fixnn = unique([intersect(Tface,Lface),intersect(Tface,Rface),...
93 intersect(Tface,Fface),intersect(Tface,Bface)]);
94 fixedUdofs = [3*fixnn-2 3*fixnn-1 3*fixnn ]; % Fixed displ.
95 freeUdofs = setdiff(allUdofs,fixedUdofs); % Free dofs for displ.
96 [U, lam1] = deal(zeros(3*nno,1),zeros(nno,1)); % lam1:Lagrange mult.
97 %% ___PART 4._____FILTER PREPARATION
98 [dy,dz,dx]=meshgrid(-ceil(rmin)+1:ceil(rmin)-1,...
99 -ceil(rmin)+1:ceil(rmin)-1,-ceil(rmin)+1:ceil(rmin)-1 );
100 h = max( 0, rmin - sqrt( dx.^2 + dy.^2 + dz.^2 ) ); % Conv. kernel
101 Hs = imfilter( ones( nely, nelz, nelx ), h); % Matrix of weights (filter)
102 %% ___PART 5._____MMA OPTIMIZATION PREPARATION & INITIALIZATION
103 [x,dVol0] = deal(zeros(nel,1),ones(nel,1)/(nel*volfrac)); % Design var. vol. cont. der
104 x(act) = (volfrac*(nel-length(NDV))-length(NDS) )/length(act); x(NDS) = 1; % Updating
105 [nMMA,mMMA,xphys,xMMA,mvLt] = deal(length(act),1,x,x(act),0.1); % Different variables
106 [xminvec,xmaxvec] = deal(zeros(nMMA,1),ones(nMMA,1)); % Min. & Max vector for MMA
107 [low, upp, xold1,xold2] = deal(xminvec,xmaxvec,xMMA,xMMA); % Low and Upp limits MMA
108 [cMMA,dMMA, a0, aMMA] = deal(1000*ones(mMMA,1),zeros(mMMA,1),1,zeros(mMMA,1));
109 dVol = imfilter(reshape(dVol0, nely, nelz, nelx)./Hs,h); % Filtered volume sensitivity
110 [loop, change] =deal(0,1);
111 %% ___PART 6._____MMA OPTIMIZATION LOOP
112 while(loop<maxit && change>0.0001)
113 loop = loop + 1; % Updating the opt. iteration
114 %___PART 6.1_____SOLVING FLOW BALANCE EQUATION
115 Kc = Kv*(1-(1-epsf)*IFprj(xphys,etaf,betaf)); % Flow coefficient
116 Dc = Ds*IFprj(xphys,etaf,betaf); % Drainage coefficient
117 Ae = reshape(Kp1(:)*Kc' + KDp1(:)*Dc',lKp1*nel,1); % Elemental flow matrix
118 AG = fsparse(IarP(:,1),IarP(:,2),Ae,[nno, nno] ); % Global flow matrix
119 Aff = AG(freePdofs,freePdofs); % AG for free pressure dofs
120 AG = AG + AG' - diag(diag(AG) ); % Determining full AG
121 PF(freePdofs) = decomposition(Aff,'ldl','lower')\(-AG(freePdofs,freePdofs)*
pfixeddofsv(:,2)); % Solving for pressure
122 PF(pfixeddofsv(:,1)) = pfixeddofsv(:,2); % Final P-field

```

```

123 %__PART 6.2_DETERMINING CONSISTENT NODAL LOADS and GLOBAL Disp. Vector
124 F = -TG*PF; % Dertmining nodal forces
125 E = Emin + xphys.^penal*(E1 - Emin); % Material interpolation
126 Ks = reshape(Ke(:)*E',lKe*nel,1); % Elemental stiffness matrix
127 KG = fsparse( Iar( :, 1 ), Iar( :, 2 ), Ks, [3*нно, 3*нно ] ); % Global stiff matrix
128 L = chol( KG( freeUdofs, freeUdofs ), 'lower' );
129 U(freeUdofs ) = L' \ ( L \ F( freeUdofs ) );
130 %__PART 6.3__OBJECTIVE, CONSTRAINT and THEIR SENSITIVITIES COMPUTATION
131 obj = U'*F; % Determining objective
132 lam1(freePdofs) = (2*U(freeUdofs)'*TG(freeUdofs,freePdofs))/Aff; % Lagrange mult.
133 objsT1 = -(E1 - Emin)*penal*xphys.^(penal - 1).*sum([U(Udofs)]*Ke0.*[U(Udofs)],2);
134 dC1k = -dIFprj(xphys,etaf,betaf).* sum((lam1(Pdofs)*(Kvs*Kp)) .* PF(Pdofs),2);
135 dC1d = dIFprj(xphys,etaf,betaf).* sum((lam1(Pdofs)*(Ds*KDp)) .* PF(Pdofs),2);
136 objsT2 = dC1k + dC1d;
137 objsens = (objsT1 + lst*objsT2); % Final sensitivities
138 Vol = sum(xphys)/(nel*volfrac)-1; % Volume fraction
139 if(loop ==1), normf = 1000/(obj);end
140 objsens = imfilter(reshape(objsens*normf, nely, nelz, nelx)./Hs,h); % Obj. sens.
141 %__PART 6.4_____SETTING and CALLING MMA OPTIMIZATION
142 xval = xMMA;
143 [xminvec, xmaxvec]= deal(max(0, xval - mvLt),min(1, xval + mvLt));
144 [xmma,~,~,~,~,~,~,~,low,upp] = mmasub(mMMA,nMMA,loop,xval,xminvec,xmaxvec,...
145 xold1,xold2,obj*normf,objsens(act),Vol,dVol(act)',low,upp,a0,aMMA,cMMA,dMMA);
146 [xold2,xold1,xnew] = deal(xold1, xval, xmma); % Updating
147 change = max(abs(xnew-xMMA)); xMMA = xnew; % Calculating chan and updating solu
148 xphys(act) = xnew;
149 xphys = imfilter(reshape(xphys, nely, nelz, nelx),h)./Hs;% Filering the Phy. vector
150 xphys = xphys(:); xphys(NDS)= 1; xphys(NDV)= 0; % Upd xphys for active/passive region
151 %__PART 6.5_____PRINTING and PLOTTING RESULTS
152 fprintf(' It.:%5i Obj.:%11.4f Vol.:%7.3f ch.:%7.3f\n',loop,obj*normf,mean(xphys),
change);
153 cla; isovals = shiftdim(reshape( xphys, nely, nelz, nelx ), 2 );
154 isovals = smooth3( isovals, 'box', 1 );
155 patch(isosurface(isovals, 0.30),'FaceColor',[0.6 0.6 0.6],'EdgeColor','none');
156 patch(isocaps(isovals, 0.30),'FaceColor','r','EdgeColor','none');
157 view( 3 ); axis equal tight off; drawnow, camlight;
158 end

```

```

%%%%%%%%%%%%%%%%%%%%%%%%%%%%%%%%%%%%%%%%%%%%%%%%%%%%%%%%%%%%%%%%%%%%%%%%
% The code, TOPress3D, is provided for pedagogical purposes. A detailed %
% description is presented in the paper:"TOPress3D: 3D topology optimization %
% with design-dependent pressure loads in MATLAB" Optimization and Engineering, %
% 2024. %
% One can download the code and its extensions for the different problems %
% from the online supplementary material and also from: %
% https://github.com/PrabhatIn/TOPress3D %
% Please send your comment to: pkumar@mae.iith.ac.in %
% One may also refer to the following four papers: %
% %
% 1. Kumar P, Frouws JS, Langelaar M (2020) Topology optimization of fluidic %
% pressure-loaded structures and compliant mechanisms using the Darcy method. %
% Structural and Multidisciplinary Optimization 61(4):1637-1655 %
% 2. Kumar P, Langelaar M (2021) On topology optimization of design-dependent %
% pressure-loaded three-dimensional structures and compliant mechanisms. %
% International Journal for Numerical Methods in Engineering 122(9):2205-2220 %
% 3. Kumar P. (2023) TOPress: a MATLAB implementation for topology optimization %
% of structures subjected to design-dependent pressure loads. %
% Structural and Multidisciplinary Optimization 66(4):97 %
% 4. Kumar P. (2023) SoRoTop: a hitchhiker's guide to topology optimization %
% MATLAB code for design-dependent pneumatic-driven soft robots %
% Optimization and Engineering: 2024 %
% %
% Disclaimer: %
% The author does not guarantee that the code is free from erros but reserves %
% all rights. Further, the author shall not be liable in any event caused by %
% use of the above mentioned code and its extensions %
% %
%%%%%%%%%%%%%%%%%%%%%%%%%%%%%%%%%%%%%%%%%%%%%%%%%%%%%%%%%%%%%%%%%%%%%%%%

```



## References

- Hammer, V.B., Olhoff, N.: Topology optimization of continuum structures subjected to pressure loading. *Structural and Multidisciplinary Optimization* **19**(2), 85–92 (2000)
- Kumar, P., Frouws, J.S., Langelaar, M.: Topology optimization of fluidic pressure-loaded structures and compliant mechanisms using the Darcy method. *Structural and Multidisciplinary Optimization* **61**(4), 1637–1655 (2020)
- Kumar, P., Langelaar, M.: On topology optimization of design-dependent pressure-loaded three-dimensional structures and compliant mechanisms. *International Journal for Numerical Methods in Engineering* **122**(9), 2205–2220 (2021)
- Sigmund, O.: A 99 line topology optimization code written in matlab. *Structural and multidisciplinary optimization* **21**(2), 120–127 (2001)
- Amir, O., Aage, N., Lazarov, B.S.: On multigrid-CG for efficient topology optimization. *Structural and Multidisciplinary Optimization* **49**(5), 815–829 (2014)
- Liu, K., Tovar, A.: An efficient 3D topology optimization code written in matlab. *Structural and Multidisciplinary Optimization* **50**(6), 1175–1196 (2014)
- Saxena, A.: Topology design with negative masks using gradient search. *Structural and Multidisciplinary Optimization* **44**(5), 629–649 (2011)
- Kumar, P.: HoneyTop90: A 90-line MATLAB code for topology optimization using honeycomb tessellation. *Optimization and Engineering* **24**(2), 1433–1460 (2023)
- Talischí, C., Paulino, G.H., Pereira, A., Menezes, I.F.: PolyTop: a matlab implementation of a general topology optimization framework using unstructured polygonal finite element meshes. *Structural and Multidisciplinary Optimization* **45**(3), 329–357 (2012)
- Kumar, P., Saxena, A.: On topology optimization with embedded boundary resolution and smoothing. *Structural and Multidisciplinary Optimization* **52**, 1135–1159 (2015)
- Chi, H., Pereira, A., Menezes, I.F., Paulino, G.H.: Virtual element method (VEM)-based topology optimization: an integrated framework. *Structural and Multidisciplinary Optimization* **62**, 1089–1114 (2020)
- Singh, N., Kumar, P., Saxena, A.: Three-dimensional material mask overlay topology optimization approach with truncated octahedron elements. *Journal of Mechanical Design* **146**(1) (2024)
- Picelli, R., Neofytou, A., Kim, H.A.: Topology optimization for design-dependent hydrostatic pressure loading via the level-set method. *Structural and Multidisciplinary Optimization* **60**(4), 1313–1326 (2019)
- Du, J., Olhoff, N.: Topological optimization of continuum structures with design-dependent surface loading—part ii: algorithm and examples for 3D problems. *Structural and Multidisciplinary Optimization* **27**, 166–177 (2004)
- Zhang, H., Liu, S.-T., Zhang, X.: Topology optimization of 3D structures with design-dependent loads. *Acta Mechanica Sinica* **26**(5), 767–775 (2010)
- Yang, X.-Y., Xie, Y.-M., Steven, G.: Evolutionary methods for topology optimisation of continuous structures with design dependent loads. *Computers & structures* **83**(12-13), 956–963 (2005)
- Sigmund, O., Clausen, P.M.: Topology optimization using a mixed formulation: an alternative way to solve pressure load problems. *Computer Methods in Applied Mechanics and Engineering* **196**(13-16), 1874–1889 (2007)

- Wang, C., Qian, X.: A density gradient approach to topology optimization under design-dependent boundary loading. *Journal of Computational Physics* **411**, 109398 (2020)
- Pinsker, J., Kumar, P., Langelaar, M., Howard, D.: Automated design of pneumatic soft grippers through design-dependent multi-material topology optimization. In: 2023 IEEE International Conference on Soft Robotics (RoboSoft), pp. 1–7 (2023). IEEE
- Pinsker, J., Wang, X., Liow, L., Xie, Y., Kumar, P., Langelaar, M., Howard, D.: Diversity-based topology optimization of soft robotic grippers. *Advanced Intelligent Systems*, 2300505 (2024)
- Wang, C., Zhao, Z., Zhou, M., Sigmund, O., Zhang, X.S.: A comprehensive review of educational articles on structural and multidisciplinary optimization. *Structural and Multidisciplinary Optimization* **64**(5), 2827–2880 (2021)
- Amir, O.: Revisiting approximate reanalysis in topology optimization: on the advantages of recycled preconditioning in a minimum weight procedure. *Structural and Multidisciplinary Optimization* **51**, 41–57 (2015)
- Aage, N., Andreassen, E., Lazarov, B.S.: Topology optimization using PETSc: An easy-to-use, fully parallel, open source topology optimization framework. *Structural and Multidisciplinary Optimization* **51**, 565–572 (2015)
- Lagaros, N.D., Vasileiou, N., Kazakis, G.: AC# code for solving 3D topology optimization problems using sap2000. *Optimization and Engineering* **20**, 1–35 (2019)
- Ferrari, F., Sigmund, O.: A new generation 99 line matlab code for compliance topology optimization and its extension to 3D. *Structural and Multidisciplinary Optimization* **62**(4), 2211–2228 (2020)
- Schmidt, S., Schulz, V.: A 2589 line topology optimization code written for the graphics card. *Computing and Visualization in Science* **14**, 249–256 (2011)
- Deng, H., Vulimiri, P.S., To, A.C.: An efficient 146-line 3D sensitivity analysis code of stress-based topology optimization written in MATLAB. *Optimization and Engineering*, 1–29 (2021)
- Zuo, Z.H., Xie, Y.M.: A simple and compact Python code for complex 3D topology optimization. *Advances in Engineering Software* **85**, 1–11 (2015)
- Fernández, E., Collet, M., Alarcón, P., Bauduin, S., Duysinx, P.: An aggregation strategy of maximum size constraints in density-based topology optimization. *Structural and Multidisciplinary Optimization* **60**, 2113–2130 (2019)
- Smith, H., Norato, J.A.: A MATLAB code for topology optimization using the geometry projection method. *Structural and Multidisciplinary Optimization* **62**(3), 1579–1594 (2020)
- Wang, Y., Kang, Z.: MATLAB implementations of velocity field level set method for topology optimization: an 80-line code for 2D and a 100-line code for 3D problems. *Structural and Multidisciplinary Optimization* **64**(6), 4325–4342 (2021)
- Du, Z., Cui, T., Liu, C., Zhang, W., Guo, Y., Guo, X.: An efficient and easy-to-extend matlab code of the Moving Morphable Component (MMC) method for three-dimensional topology optimization. *Structural and Multidisciplinary Optimization* **65**(5), 158 (2022)
- Zhao, Y., Guo, G., Zuo, W.: Matlab implementations for 3D geometrically nonlinear topology optimization: 230-line code for SIMP method and 280-line code for MMB method. *Structural and Multidisciplinary Optimization* **66**(7), 146 (2023)

- Zhuang, C., Xiong, Z., Ding, H.: An efficient 2D/3D NURBS-based topology optimization implementation using page-wise matrix operation in MATLAB. *Structural and Multidisciplinary Optimization* **66**(12), 1–23 (2023)
- Kim, D., Ji, Y., Lee, J., Yoo, J., Min, S., Jang, I.G.: A MATLAB code of node-based topology optimization in 3D arbitrary domain for additive manufacturing. *Structural and Multidisciplinary Optimization* **65**(11), 311 (2022)
- Kumar, P.: TOPress: a MATLAB implementation for topology optimization of structures subjected to design-dependent pressure loads. *Structural and Multidisciplinary Optimization* **66**(4) (2023)
- Svanberg, K.: The method of moving asymptotes—a new method for structural optimization. *Int J Numer Meth Eng* **24**(2), 359–373 (1987)
- Engblom, S., Lukarski, D.: Fast matlab compatible sparse assembly on multicore computers. *Parallel Computing* **56**, 1–17 (2016)
- Kumar, P., Langelaar, M.: Topological synthesis of fluidic pressure-actuated robust compliant mechanisms. *Mechanism and Machine Theory* **174**, 104871 (2022)
- Kumar, P.: Towards Topology Optimization of Pressure-Driven Soft Robots. In: *Conference on Microactuators and Micromechanisms*, pp. 19–30 (2022). Springer
- Kumar, P., Saxena, A.: An improved material mask overlay strategy for the desired discreteness of pressure-loaded optimized topologies. *Structural and Multidisciplinary Optimization* **65**(10), 304 (2022)
- Banh, T.T., Shin, S., Kang, J., Lee, D.: Frequency-constrained topology optimization in incompressible multi-material systems under design-dependent loads. *Thin-Walled Structures* **196**, 111467 (2024)
- Kumar, P.: Topology optimization of pressure-loaded multi-material structures. In: *Advances in Structural Integrity for Mechanical, Civil, and Aerospace Applications* (2024). Springer
- Kumar, P.: SoRoTop: a hitchhiker’s guide to topology optimization MATLAB code for design-dependent pneumatic-driven soft robots. *Optimization and Engineering*, 1–35 (2023)
- Bruns, T.E., Tortorelli, D.A.: Topology optimization of non-linear elastic structures and compliant mechanisms. *Comput Method Appl Mech Eng* **190**(26-27), 3443–3459 (2001)
- Zienkiewicz, O.C., Taylor, R.L., Zhu, J.Z.: *The Finite Element Method: Its Basis and Fundamentals*. Elsevier, (2005)